Hindawi Publishing Corporation
Mathematical Problems in Engineering
Volume 2016, Article ID 2834192, 9 pages
http://dx.doi.org/10.1155/2016/2834192

Research Article

The Analysis of the Concrete Gravity Dam's Foundation Uplift Pressure under the Function of Typhoon

Kai Zhu,[1,2,3] Chongshi Gu,[1,2,3] Jianchun Qiu,[1,2,3] and Hao Li[1,2,3]

[1]*State Key Laboratory of Hydrology-Water Resources and Hydraulic Engineering, Hohai University, Nanjing 210098, China*
[2]*National Engineering Research Center of Water Resources Efficient Utilization and Engineering Safety, Hohai University, Nanjing 210098, China*
[3]*College of Water-Conservancy and Hydropower, Hohai University, Nanjing 210098, China*

Correspondence should be addressed to Kai Zhu; 879058923@qq.com

Received 22 October 2015; Revised 29 February 2016; Accepted 9 March 2016

Academic Editor: Dan Simon

How to evaluate the seepage safety status of the concrete gravity dam under the function of short-period heavy rainfall and the possible historical extreme reservoir water level during typhoon is an important issue considering the dam safety-monitoring. Based on analysis of the monitoring series of the foundation uplift pressure, this paper assumed the influential process of antecedent reservoir water level and rainfall as a process of normal distribution and introduced the mutation factor to reflect the uprush feature of uplift pressure under the function of high-influential typhoon. Moreover, the corresponding hysteresis days and influential days of the model are optimized with quantum genetic algorithm (QGA) to raise the fitting and prediction accuracy. It is verified that the new statistical model for fitting can obtain higher multiple correlation coefficient (0.972) compared with the traditional statistical model (0.925) and could also perfectly predict the uprush feature of the pressure during the typhoon, which is of certain theoretical and practical application value in the future.

1. Introduction

Under the effects of global warming, extremely abnormal climate events have occurred with increasing frequency in recent years and have threatened the safe operation of hydraulic structures everywhere [1, 2]. Among these events, typhoons are particularly remarkable. Typhoons are among the most common natural disasters and are characterized by high occurrence frequency, abruptness, wide influential range, and strong disaster intensity. Every year, China encounters 8-9 typhoons with strong winds (especially in the southeast coastal areas) and is among the countries that experience the most typhoon landfalls and suffer the worst damage [3–5]. As a result of the earth's deteriorating environmental condition, the occurrence tendency of this disastrous weather event is on the rise [6, 7]. For example, on June 11, 2014, typhoon "Haima" landed on Guangdong, Guangxi, and Hainan and caused heavy storms and, particularly, torrential rainstorms in the coastal cities located in south Meizhou, west of the Pearl River Delta, and west Guangdong. The rainfall was between 50 mm and 250 mm, and the maximum cumulative rainfall was 377.6 mm in Xinhui District. The rainstorm increased the water storage of 32 large reservoirs in Guangdong by 56 million m^3. On October 7, 2013, typhoon "Fitow" landed at Shacheng Town, Fuding City, Fujian Province, China, and was the strongest typhoon hitting China during the month of October since 1949. During the flood period, the Yongjiang basin encountered the strongest rainfall in the hydrological history, causing severe waterlogging in Ningbo City and resulting in widespread and long-term interruption of traffic and power. The average rainfall of the city was 187.8 mm and the maximum single-station rainfall reached up to 417.5 mm. On June 18, 2014, super typhoon "Wilson" landed on Hainan, Guangdong, and Guangxi successively and was the strongest typhoon in those areas during the past 41 years. According to statistics, the average rainfall in Hainan on June 18 was 264 mm, and the rainfall in Changjiang and Haikou City was greater than 500 mm, causing the water storage of all

reservoirs in Hainan to increase by 0.318 billion m^3, and 241 reservoirs took urgent measures to discharge flooding. The extreme weather conditions of strong winds, heavy rainfall, and storm-tides that accompany typhoons can increase the frequency and intensity of hydrological extremes, which lead to extraordinary flooding and new historical extreme water levels, thus adding to the working risk of hydraulic engineering [8, 9]. Furthermore, the heavy rainfall during typhoons can lead to geologic hazards and deteriorate material properties of dam bodies, which in turn reduce the projects' service lives.

The seepage safety evaluation of a concrete gravity dam is the main task of dam security monitoring. For a gravity dam of 100 m, the foundation uplift pressure is approximately 20% of the dam weight under normal reservoir level and is therefore the main load for concrete gravity dams which directly influences the dam stability [10, 11]. Conventional statistical models decompose the uplift pressure into water level component, rainfall component, temperature component, and aging component and consider the foundation uplift pressure to be linearly correlated with the average value of the antecedent water level and rainfall [12]. It is analyzed from the monitoring data that the foundation uplift pressure during typhoon increases sharply under the function of short-duration heavy rainfall and historical extreme reservoir water level, while the traditional statistical model cannot reflect the feature. The reason is that the traditional statistical model adopts the mean value of water level and rainfall of the past i days to fit the foundation uplift pressure, which would weaken the effects of historical extreme water level and rainfall. Besides, the four components that constitute the traditional model are designed to fit the long-period monitoring series and cannot reflect the sudden decrease of antipermeability of dam foundation system during the typhoon.

Based on analysis of concrete gravity dam's seepage characteristic, this paper proposes a novel statistical model of foundation uplift pressure considering the nonlinear influence of antecedent reservoir water level and rainfall and introduces the mutation factor to simulate the uprush feature of the pressure during typhoon. The quantum genetic algorithm (QGA) is adopted to optimize the model parameters to raise the corresponding fitting and prediction accuracy. To verify the feasibility of the proposed method, a certain concrete gravity dam in Fujian Province is chosen as an example. By comparing with the monitoring values and the results of traditional statistical model, the new statistical model for fitting is proved to have higher fitting accuracy and can also accurately predict the uplift pressure during the typhoon Fitow in 2013.

2. Basic Theory

2.1. The Statistical Model of Foundation Uplift Pressure of Concrete Gravity Dam. The foundation uplift pressure of concrete gravity dam is mainly influenced by the reservoir water level, rainfall, bedrock temperature, and time-varying characteristic of dam-material [13]. In order to reflect the uprush feature of the pressure during typhoon, the mutation factor is introduced in this paper. Therefore, the statistical model of the foundation uplift pressure is as follows:

$$P = P_H + P_R + P_\theta + P_T + P_M. \tag{1}$$

In the formula, P represents dam piezometric-tube level; P_H represents water level component; P_R represents the rainfall component; P_θ represents time-varying component; P_T represents temperature component; and P_M represents the mutation factor.

(1) Water Level Component P_H. Unlike the traditional model considering the influential process of the antecedent reservoir water level as an "average" process (Figure 1), this paper assumed the process as a process of normal distribution [12], as is shown in Figure 2, and the corresponding form of the component is as follows:

$$\begin{aligned} P_H &= \sum_{j=1}^{m_1} a_j \left[\int_{-\infty}^{0} \frac{1}{\sqrt{2\pi}} e^{-(t-x_1)^2/2x_2^2} H_i(t)\, dt \right]^j \\ &= \sum_{j=1}^{m_1} a_j \left[H_{um} \right]^j, \end{aligned} \tag{2}$$

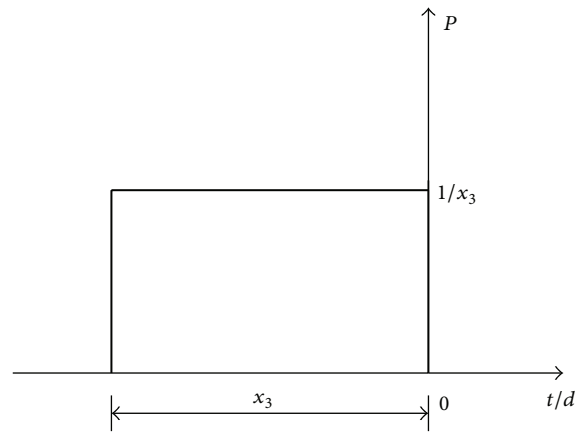

Figure 1: Average distribution influential curve.

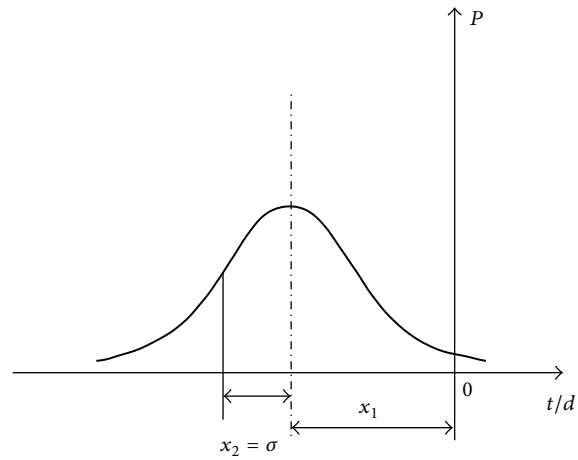

Figure 2: Normal distribution influential curve.

where a_j is the regression coefficient; x_1 and x_2 are the hysteresis and influential days; $H_i(t)$ and H_{um} are the actual and effective reservoir water-level, respectively.

Among them, x_1 and x_2 should be calculated by trial and the discrete integral should be adopted since the reservoir water level is generally measured one time a day.

(2) Rainfall Component P_R. The influential process of rainfall shows a significantly nonlinear feature and there is also hysteresis effect [13]. According to the influential laws of rainfall on groundwater and exponential law of fracture seepage, the form of rainfall component is taken as follows:

$$P_R = \sum_{i=1}^{m_2} b_i \left[\int_{-\infty}^{0} \frac{1}{\sqrt{2\pi} x_4} e^{-(t-x_3)/2x_4^2} \left[R(t)\right]^{2/5} dt \right]^i = \sum_{i=1}^{m_2} b_i \left[R_{um}\right]^i, \tag{3}$$

where b_j is the regression coefficient; x_3 and x_4 represent the hysteresis and influential days; $R(t)$ and R_{um} are the actual and effective rainfall, respectively.

Similarly, x_3 and x_4 should also be obtained by trial and the continuous integration should be replaced by discrete integral.

(3) Temperature Component P_T. The foundation seepage is closely related with the variations of ground fractures while the fracture variation is highly affected by the bedrock temperature [14]. In this paper, the periodic function is adopted to represent the temperature component as follows:

$$P_T = \sum_{i=1}^{2} \left(c_{1i} \sin \frac{2\pi i t}{365} + c_{2i} \cos \frac{2\pi i t}{365} \right), \tag{4}$$

where c_{1i} and c_{2i} are the regression coefficients.

(4) Time-Varying Factor P_θ. The basic form of the component is as follows [14, 15]:

$$P_\theta = d_1 \theta + d_2 \ln \theta, \tag{5}$$

where d_1 and d_2 are the regression coefficients; θ is the number of monitoring days from the initial reservoir impoundment divided by 100.

(5) Mutation Factor. When the measured reservoir water level or rainfall exceeds the historical maximum water level or rainfall, the factor is introduced into the model. The mutation factor is directly related with the maximum value of environmental variables and the corresponding excess compared with the historical maximum values. Based on this, the mutation factor is defined as follows:

$$P_M = \sum_{i=1}^{2} e_i \left(DH_i\right). \tag{6}$$

In the formula, e_i represents the regression coefficient; DH_1 represents the product of extreme reservoir water level H and its excess ΔH during the typhoon; DH_2 represents the product of extreme rainfall R and its excess ΔR.

In summary, the novel statistical model of uplift pressure for concrete gravity dam considering the effect of high-influential typhoon is denoted as follows:

$$P = \sum_{j=1}^{m_1} a_j \left[R_{um}\right]^j + \sum_{j=1}^{m_2} b_j \left[R_{um}\right]^j + \sum_{i=1}^{2} \left(c_{1i} \sin \frac{2\pi i t}{365} + c_{2i} \cos \frac{2\pi i t}{365} \right) + d_1 \theta + d_2 \ln \theta + \sum_{i=1}^{2} e_i \left(DH_i\right). \tag{7}$$

2.2. Quantum Genetic Algorithm. In 1982, Richard Feynman and Benioff firstly put forward the concept of quantum computing based on quantum mechanical properties. In 1985, Deutsch [16] indicated that the concurrent quantum computation can be realized by using the coherent-superposition property of quantum states and defined the first quantum calculation model. Shor [17] proposed the first quantum algorithm based on the quantum concurrent computation in 1994 and used it to solve the large prime factorization. In 1996, Grover [18] proposed a quantum algorithm for random database search. In 2002, Han and Kim firstly put forward the quantum genetic algorithm (QGA) based on quantum theory [19]. QGA is a probability search algorithm by encoding the chromosomes with quantum bits and conducting the evolutionary search by updating the population with quantum gate based on the information of current best individual [20, 21]. Compared with the traditional evolutionary algorithm, QGA can strike a balance between exploration and development and have the property of small population size, fast convergence speed, and global optimization ability [22, 23].

The basic information unit in QGA is called quantum bit and the state of a quantum bit can be expressed as follows [24]:

$$\left|\varphi\right\rangle = \alpha \left|0\right\rangle + \beta \left|1\right\rangle, \tag{8}$$

where α and β represent the probability amplitudes of the corresponding quantum bit and they also meet the normalized criterion as follows:

$$|\alpha|^2 + |\beta|^2 = 1. \tag{9}$$

Thus, the state of a quantum bit can also be denoted as follows:

$$\left|\varphi\right\rangle = \cos \frac{\theta}{2} \left|0\right\rangle + e^{i\varphi} \sin \frac{\theta}{2} \left|1\right\rangle. \tag{10}$$

In the quantum genetic algorithm, quantum information is encoded by pairs of complex numbers [25] and the quantum chromosome composed of m sets of quantum bits can be expressed as follows:

$$\left[\begin{array}{c|c|c|c} \alpha_1 & \alpha_2 & \cdots & \alpha_m \\ \beta_1 & \beta_2 & \cdots & \beta_m \end{array} \right], \tag{11}$$

where $|\alpha_i|^2 + |\beta_i|^2 = 1$ $(i = 1, 2, \ldots, m)$.

Table 1: $f(\alpha_i, \beta_i)$ value query table.

d_1	d_2	$f(\alpha_i, \beta_i)$	
$d_1 > 0$	$d_2 > 0$	$\lvert\xi_1\rvert > \lvert\xi_2\rvert$	$\lvert\xi_1\rvert < \lvert\xi_2\rvert$
True	True	+1	−1
True	False	+1	+1
False	True	−1	−1
False	False	−1	+1

The encoding method can represent the random linear superposition of quantum states. For example, a chromosome with 3 quantum bits can be expressed as follows:

$$\begin{bmatrix} \frac{1}{\sqrt{2}} & \frac{\sqrt{3}}{2} & \frac{1}{2} \\ \frac{1}{\sqrt{2}} & \frac{1}{2} & \frac{\sqrt{3}}{2} \end{bmatrix}. \tag{12}$$

The update of quantum gate can be denoted as [26]

$$\begin{bmatrix} \alpha_i' \\ \beta_i' \end{bmatrix} = U(\theta_i) \begin{bmatrix} \alpha_i \\ \beta_i \end{bmatrix} = \begin{bmatrix} \cos(\theta_i) & -\sin(\theta_i) \\ \sin(\theta_i) & \cos(\theta_i) \end{bmatrix} \begin{bmatrix} \alpha_i \\ \beta_i \end{bmatrix}, \tag{13}$$

where $U(\theta_i) = \begin{bmatrix} \cos(\theta_i) & -\sin(\theta_i) \\ \sin(\theta_i) & \cos(\theta_i) \end{bmatrix}$ is quantum rotating gate, among which the variables can be expressed as follows:

$$\begin{aligned} \theta_i &= k \cdot f(\alpha_i, \beta_i), \\ k &= \pi \cdot \exp\left(-\frac{t}{\text{iter}_{\max}}\right), \end{aligned} \tag{14}$$

where k is the adaptive variable; t is the evolutionary population; $\text{iter}_{\max}$ is a constant depending on the complexity of the optimization problem.

The search strategy of $f(\alpha_i, \beta_i)$ is shown in Table 1. In the table, α_1 and β_1 are the probability amplitude of global optimal solution, $d_1 = \alpha_1 \times \beta_1$ and $\xi_1 = \tan^{-1}(\beta_1/\alpha_1)$; α_2 and β_2 are the probability amplitude of current solution, $d_2 = \alpha_2 \times \beta_2$ and $\xi_2 = \tan^{-1}(\beta_2/\alpha_2)$. If both d_1 and d_2 are greater than 0, the current solution and global optimal solution will be in the first quadrant or third quadrant. When $|\xi_1| > |\xi_2|$, the current solution should be rotated counterclockwise, $f(\alpha_i, \beta_i) = +1$; otherwise, $f(\alpha_i, \beta_i) = -1$. Similarly, the other three rotational criteria can be deduced by the same way.

Furthermore, in order to prevent the optimization process from converging at local extremum, the algorithm also introduces the mutation operator based on certain probability. For instance, a quantum bit $\alpha|0\rangle + \beta|1\rangle$ can be transformed into $\alpha|1\rangle + \beta|0\rangle$ through the operation. In practice, the mutation probability is generally taken between 0.1 and 0.01, which can both maintain the diversity of the population and prevent the algorithm from converging at local extremum.

In this paper, the stepwise regression algorithm is adopted to fit the monitoring series of foundation uplift pressure and the corresponding multiple correlation coefficient is taken as the fitness value. The basic steps of the algorithm are shown in Figure 3.

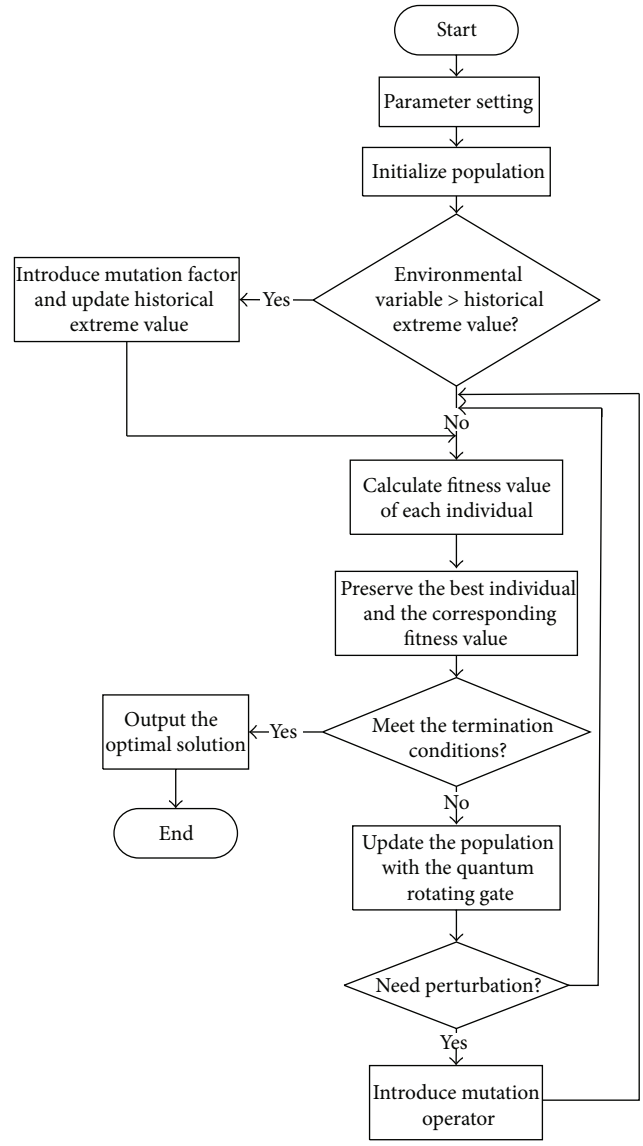

Figure 3: Flow chart of quantum genetic algorithm.

3. Case Study

3.1. Project Introduction. A hydropower station, which is located at the upstream of Yao River in Fujian Province, is taken as an example. The station is a first-class hub project and is mainly composed of roller compacted concrete gravity dam, Huyangli auxiliary dam, spillway, bottom flood-releasing outlets, water-conveyance structures in left bank, and the underground powerhouse. The highest elevation of dam crest is 179.0 m and the total length of dam crest is 300 m. The normal water level and check flood level of reservoir are 173.0 m and 177.8 m with the corresponding regulating capacity and the total capacity of 1.122 billion m^3 and 2.035 billion m^3, respectively. The downstream view of the concrete gravity dam is shown in Figure 4.

To monitor the dam seepage condition, 126 osmometers, 9 seepage-measuring weirs, 46 dam foundation piezometer-tubes, 11 observation wells, and 131 hydraulic bases are

installed by the constructors. The layout of the seepage-monitoring instruments in 4 # dam section is shown in Figure 5. The analysis of the monitoring values shows that the uplift pressure of A6-UP-01 measurement point is at high level each year and has obvious uprush phenomenon during the typhoon. Therefore, this paper will focus on analysis of the point with the new statistical model.

3.2. The Fitting of the Foundation Uplift Pressure. The monitoring series of A6-UP-01, A6-UP-02, and A6-UP-04 from Oct. 1, 2008, to Oct. 3, 2013, are selected as the original data. The initial historical extreme values of reservoir water level and rainfall are taken as 176.4 m and 235 mm, respectively. The maximum number of iterations of QGA is taken as 2000. When the iterations of the algorithm exceed 2000 or the multiple correlation coefficient is over 0.99, the algorithm is terminated. The traditional genetic algorithm (GA) is also adopted to verify the effectiveness of QGA. The evolution of the fitness value of three measurement points is shown in Figure 6.

As far as the measurement point A6-UP-01 is considered, the fitness value of QGA is stable at 0.972 after 1316 generations while the GA is only stable at 0.961 after 1589 generations; the fitness value of QGA for A6-UP-02 measurement point finally converges to 0.96 with 784 generations corresponding to 0.953 of GA with 1326 generations; the fitness value of QGA for A6-UP-04 measurement point finally converges to 0.971 with 687 generations while the GA only converges to 0.968 after 1213 generations.

Therefore, it is clear that the convergence speed of quantum genetic algorithm (QGA) is remarkably improved and the premature phenomenon can be effectively avoided compared with the traditional genetic algorithm (GA). The QGA can always converge to a higher fitness value in fewer generations than GA.

The conventional statistical model of the foundation uplift pressure of concrete gravity dam is also introduced in this paper to verify the effectiveness of the proposed method and the formula of the model is as follows:

$$P = \sum_{i=1}^{m_1} a_{ui}\overline{H}_{ui} + \sum_{i=1}^{m_2} b_i\overline{p}_i + \sum_{i=1}^{m_3}\left(c_{1i}\sin\frac{2\pi it}{365} + c_{2i}\cos\frac{2\pi it}{365}\right) + d_1\theta + d_2\ln\theta + a_0, \tag{15}$$

where a_{ui} is the regression coefficient of reservoir water level; $\overline{H}_{ui}$ is the average water level of former i days; b_i is the regression coefficient of rainfall; $\overline{p}_i$ is average rainfall of former i days; c_{1i} and c_{2i} are regression coefficients of the temperature component; d_1 and d_2 are the regression coefficients of the aging component.

In this paper, the traditional method is conducted by fitting the monitoring values of A6-UP-01 with stepwise regression method based on the conventional statistical model by taking $m_1 = m_2 = m_3 = 5$. The fitting results of the two methods are shown in Figure 7.

It is obvious that the proposed method can perfectly simulate the variation of the foundation uplift pressure and

Figure 4: The downstream view of the concrete gravity dam.

the fitting results of the proposed method are more accurate to the monitoring values compared with the conventional statistical model. Moreover, as the novel model in this paper considers the nonlinear influence of antecedent reservoir water level and rainfull, the proposed method can perfectly reflect the uprush feature of the pressure and is close to the recorded value at the top of the monitoring series. The multiple correlation coefficient of the traditional statistical model is 0.925 and is far less than 0.972 of the new statistical model in this paper. Therefore, it can be concluded that the proposed model possesses higher fitting precision than the traditional statistical model.

The novel statistical model of the foundation uplift pressure for measurement point A6-UP-01 can thus be established through the above steps and the hysteretic days and influential days of the upstream water level and rainfall are 3 d and 63 d and 4 d and 52 d, respectively.

Therefore, the obtained components of foundation uplift pressure are as follows.

(1) Water Level Component. Consider

$$P_H = 0.086H_{um}^5 - 7.174H_{um}^4 + 78.355H_{um}^3 - 803.41H_{um}^2 + 2707.147H_{um}. \tag{16}$$

(2) Rainfall Component. Consider

$$P_R = -147.56R_{um}^5 + 407.749R_{um}^4 - 565.423R_{um}^3 + 479.507R_{um}^2 - 227.248R_{um}. \tag{17}$$

(3) Temperature Component. Consider

$$P_T = 0.602\sin\frac{2\pi t}{365} - 16.972\sin\frac{4\pi t}{365} + 6.563\cos\frac{2\pi t}{365} - 1.318\cos\frac{4\pi t}{365}. \tag{18}$$

(4) Aging Component. Consider

$$P_\theta = -30.741\theta + 0.443\ln\theta. \tag{19}$$

(5) Mutation Factor. Consider

$$P_E = 0.081\,(DH)^5 - 3.785\,(DH)^4 + 14.421\,(DH)^3 - 61.702\,(DH)^2 + 129.017\,(DH). \tag{20}$$

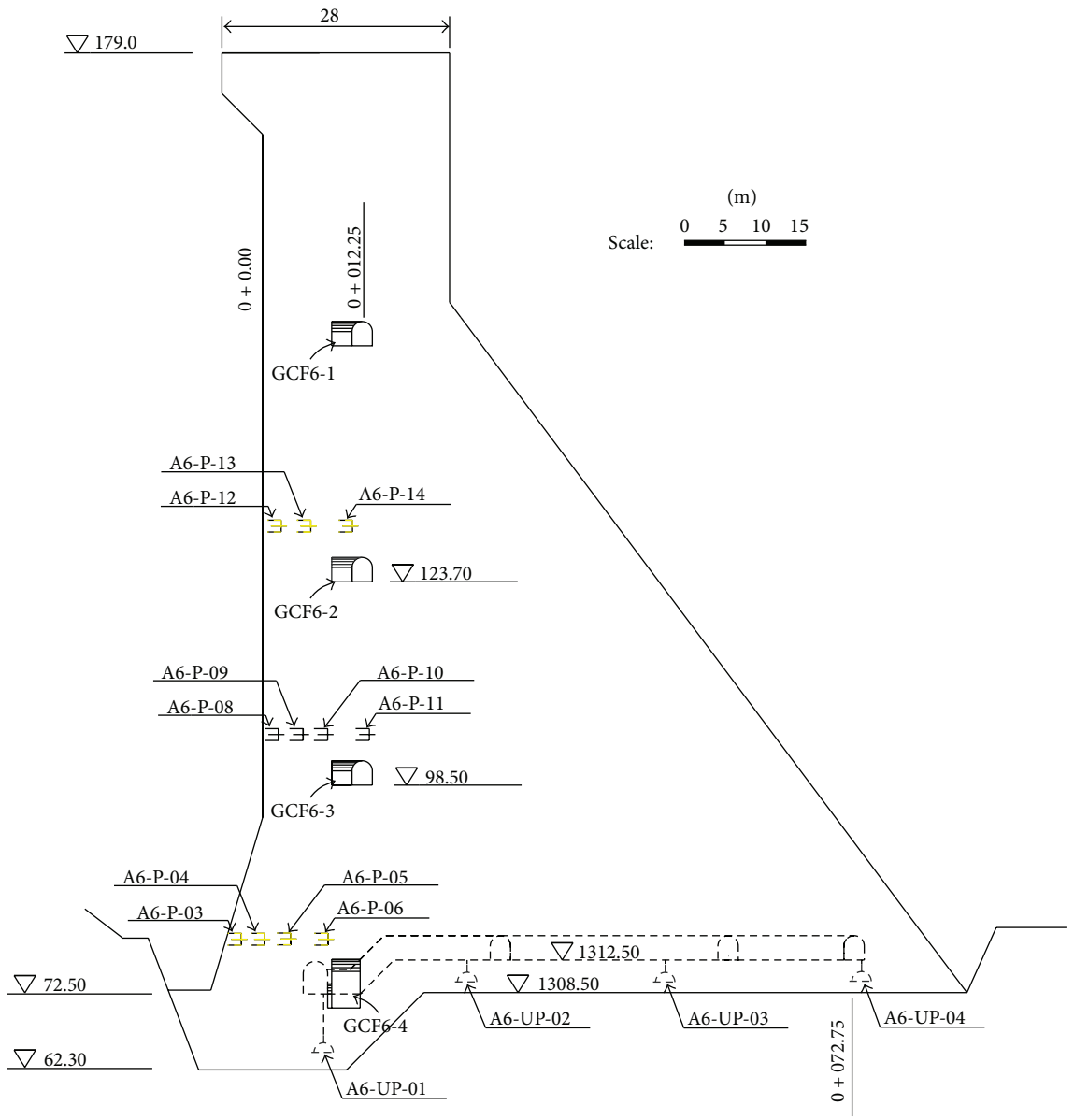

Figure 5: The layout of the seepage-monitoring instruments in 4 # dam section.

3.3. The Analysis of the Foundation Uplift Pressure during the Typhoon Fitow

3.3.1. The Qualitative Analysis of the Foundation Uplift Pressure. In 2013, the 23rd tropical storm, Fitow typhoon, formed in the east ocean of the Philippines at 20:00 on Sep. 30 and the storm center was located at north latitude 13.9° and east longitude 132.5°. At 17 pm on Oct. 1, Fitow typhoon intensified into a strong tropical storm and then developed into a typhoon in the early morning of Oct. 3 and finally changed into a powerful typhoon in the afternoon of Oct. 4. When Fitow typhoon landed on China in Shacheng Town, Fuding City, Fujian Province, at 1:15 on Oct. 7, the largest wind scale of the center was 14th (18 m/s) and the center minimum pressure was 955 hectopascal, which posed a great pressure for the safety operating of the hydraulic structures in the area.

During the typhoon, the area encountered the strongest rainfall in hydrological history. The process of the areal rainfall from Oct. 5, 2013, to Oct. 9, 2013, is shown in Figure 8. The area suffered from a continuous rainfall, occasionally heavy to torrential rain during the typhoon. The rainfall concentrated on Oct. 6 and 7 and the areal rainfall of these two days reached up to 507.2 mm. The total rainfall during the typhoon reached up to 565.2 mm, which is close to the once-in-a-century rainfall of the area.

Under the function of the typhoon Fitow, the reservoir water level reached the historical maximum value of 177.6 m on Oct. 10, which brought a severe challenge for the safe operation of the dam.

The monitoring values of the uplift pressure of each measurement point in 4 # dam section from Oct. 5 to Oct. 21 are shown in Figure 9. As is shown in the figure, the uplift

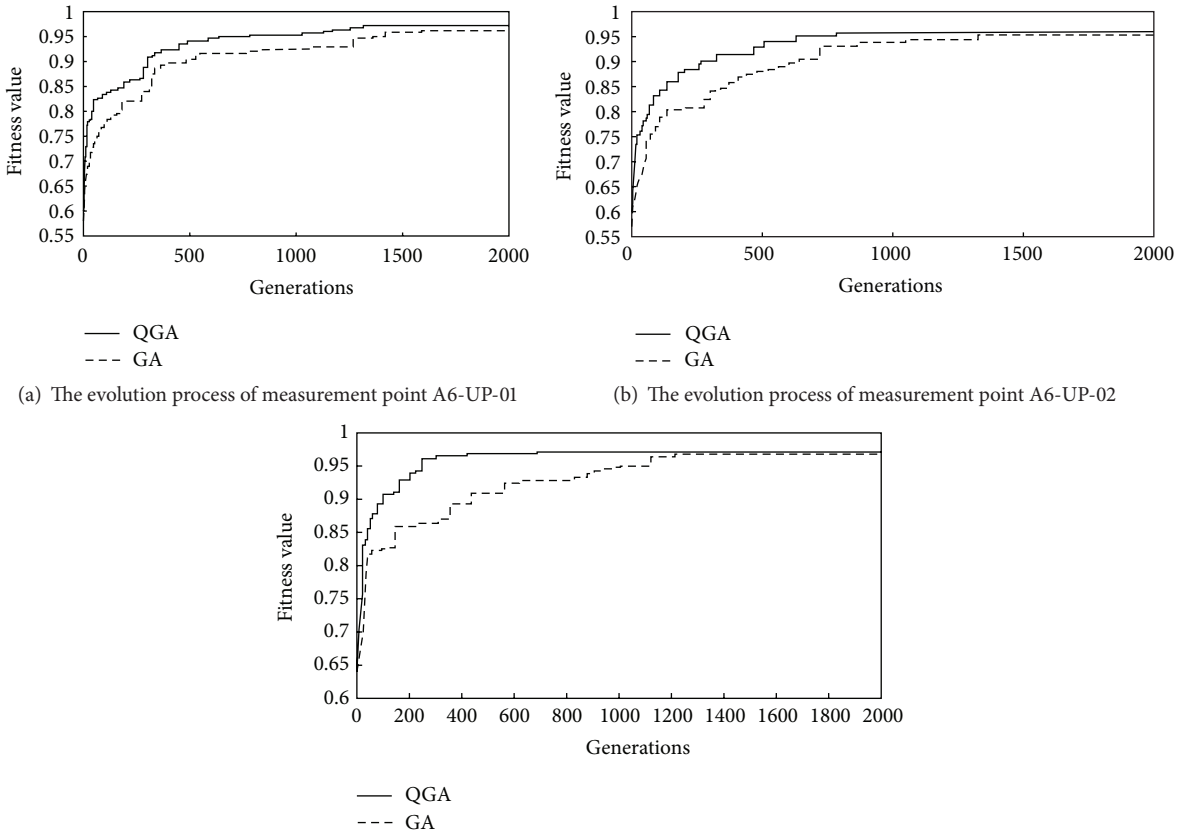

(a) The evolution process of measurement point A6-UP-01

(b) The evolution process of measurement point A6-UP-02

(c) The evolution process of measurement point A6-UP-04

Figure 6: The evolution process of the best individual's fitness value of the three measurement points.

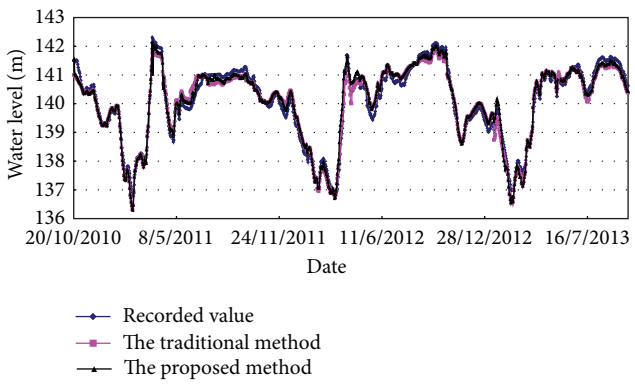

Figure 7: Fitting results of the proposed method.

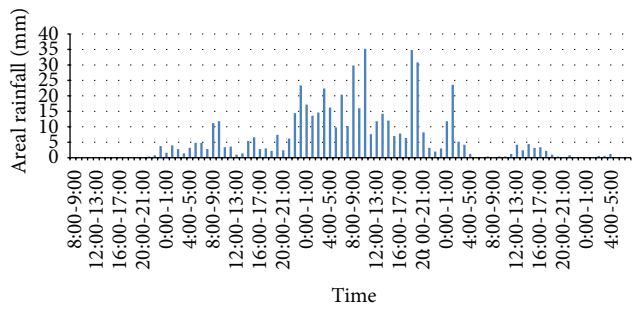

Figure 8: The areal rainfall process during the typhoon Fitow.

pressure of each measurement point increased obviously from Oct. 7 after the typhoon Fitow landed on China, except for A6-UP-03. The monitoring values of A6-UP-01 and A6-UP-02 reached the peak value on Oct. 8 while the A6-UP-04 showed more obvious hysteresis effect and reached the peak value around Oct. 10. After that, the monitoring values of each point gradually returned to normal while the reservoir water level dropped. Among the four measurement points, the values of A6-UP-01 were obviously higher than the other points, with its maximum value of 141.93 m on Oct. 8 during the typhoon. Therefore, the paper would focus on the seepage safety analysis of the point with the new statistical model.

3.3.2. The Prediction of Foundation Uplift Pressure during Typhoon Fitow. In this paper, the established model above is applied to forecast the uplift pressure of the A6-UP-01 measurement point from Oct. 5, 2013, to Oct. 30, 2013, during the Typhoon Fitow. The historical extreme water level H_{max} and rainfall R_{max} are updated as 176.9 m and 279.2 mm, respectively. The predicted results of the two methods are shown in Figure 10.

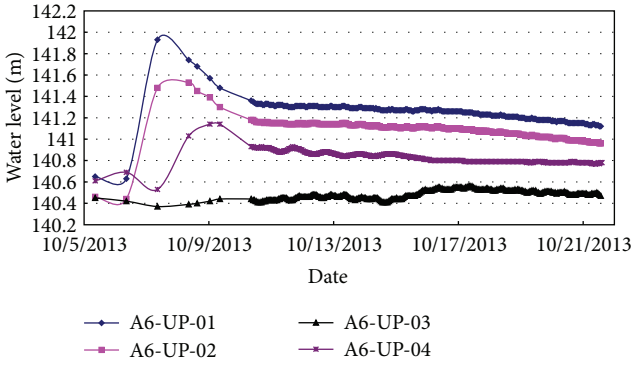

Figure 9: The process line of the foundation uplift pressure of 4 # dam section.

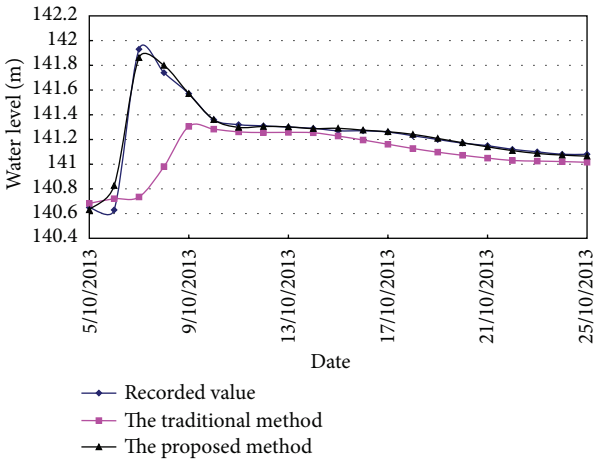

Figure 10: The comparison of the predicted value of the piezometric water level.

As is shown in Figure 10, by introducing the mutation factor into the statistical model, the proposed method can perfectly predict the uprush phenomenon of the foundation uplift pressure during the typhoon Fitow and the predicted value is rather close to the monitoring values throughout the period. On the other hand, as the traditional statistical model cannot reflect the function of short-period heavy rainfall and historical extreme reservoir water level, the traditional model can hardly simulate the sharp variation of uplift pressure and is only close to the monitoring values after the typhoon passed away.

4. Conclusion

This paper proposes the novel statistical model of the foundation uplift pressure considering the nonlinear influences of the antecedent environmental variables and introduces the mutation factor to simulate the uprush feature of the pressure under the function of typhoon. By comparing with traditional statistical model, the following conclusions could be drawn:

(1) The short-duration heavy rainfall and historical extreme reservoir water-level during the typhoon would remarkably raise the operating risk of hydraulic project. How to synthetically evaluate the safety status of the dam under the condition would be an important subject in the future.

(2) As far as the measurement point A6-UP-01 is considered, the new statistical model is proved to have better fitting accuracy and can also accurately predict the uprush feature of the foundation uplift pressure during the typhoon compared with the traditional statistical model.

(3) The optimization process of the QGA possesses good property of fast convergence speed and global optimization ability which can effectively avoid falling into local extremum of GA.

Competing Interests

The authors declare that they have no competing interests.

Acknowledgments

This work was supported by the National Natural Science Foundation of China (Grant nos. 41323001, 51409018, 51139001, and 51379068), Research Fund for the Doctoral Program of Higher Education of China (Grant nos. 20120094110005, 20120094130003, and 20130094110010), Program for New Century Excellent Talents in University (Grant no. NCET-11-0628), the Ministry of Water Resources Public Welfare Industry Research Special Fund Project (Grant nos. 201201038 and 201301061), and the Open Foundation of Key Laboratory of Earth-Rock Dam Failure Mechanism and Safety Control Techniques of Ministry of Water Resources (Grant nos. YK914022).

References

[1] Z.-M. Fu, Y. Xiang, C.-D. Liu, Z.-Y. Li, and Z.-J. Wang, "Resilience of hydraulic structures under significant impact of typhoons," *Water Science and Engineering*, vol. 4, no. 3, pp. 284–293, 2011.

[2] J. Lubchenco and T. R. Karl, "Predicting and managing extreme weather events," *Physics Today*, vol. 65, no. 3, pp. 31–37, 2012.

[3] Y. Xiang, Z. Fub, H. Yuana, Z. Wanga, and Y. Guana, "Effect of climate anomaly on xixi roller compacted concrete gravity dam," *Procedia Earth and Planetary Science*, vol. 5, pp. 13–18, 2012.

[4] L. Li, A. Kareem, Y. Xiao, L. Song, and C. Zhou, "A comparative study of field measurements of the turbulence characteristics of typhoon and hurricane winds," *Journal of Wind Engineering and Industrial Aerodynamics*, vol. 140, pp. 49–66, 2015.

[5] Y. Li, D. Li, J. Fang et al., "Impact of Typhoon Morakot on suspended matter size distributions on the East China Sea inner shelf," *Continental Shelf Research*, vol. 101, pp. 47–58, 2015.

[6] W.-P. Huang, C.-A. Hsu, C.-S. Kung, and J. Z. Yim, "Numerical studies on typhoon surges in the Northern Taiwan," *Coastal Engineering*, vol. 54, no. 12, pp. 883–894, 2007.

[7] L.-F. Hsiao, M.-J. Yang, C.-S. Lee et al., "Ensemble forecasting of typhoon rainfall and floods over a mountainous watershed in Taiwan," *Journal of Hydrology*, vol. 506, pp. 55–68, 2013.

[8] N.-S. Hsu, C.-L. Huang, and C.-C. Wei, "Multi-phase intelligent decision model for reservoir real-time flood control during typhoons," *Journal of Hydrology*, vol. 522, pp. 11–34, 2015.

[9] G.-F. Lin, P.-Y. Huang, and G.-R. Chen, "Using typhoon characteristics to improve the long lead-time flood forecasting of a small watershed," *Journal of Hydrology*, vol. 380, no. 3-4, pp. 450–459, 2010.

[10] G. A. Plizzari, "On the influence of uplift pressure in concrete gravity dams," *Engineering Fracture Mechanics*, vol. 59, no. 3, pp. 253–267, 1998.

[11] F. Yan, T. Xinbin, and G. Li, "The uplift mechanism of the rock masses around the Jiangya dam after reservoir inundation, China," *Engineering Geology*, vol. 76, no. 1-2, pp. 141–154, 2004.

[12] Z. Wu, *Safety Monitoring Theory & Its Application of Hydraulic Structures*, Higher Education Press, Beijing, China, 2003.

[13] H. Su and X. Sun, *Comprehensive Evaluation and Tendency Prediction Model for Concrete Dam Seepage Behavior*, Yangtze River, China, 2013.

[14] M. Tatin, M. Briffaut, F. Dufour, A. Simon, and J.-P. Fabre, "Thermal displacements of concrete dams: accounting for water temperature in statistical models," *Engineering Structures*, vol. 91, pp. 26–39, 2015.

[15] H. Su, Z. Wen, J. Hu, and Z. Wu, "Evaluation model for service life of dam based on time-varying risk probability," *Science in China, Series E: Technological Sciences*, vol. 52, no. 7, pp. 1966–1973, 2009.

[16] D. Deutsch, "Quantum theory, the church-turing principle and the universal quantum computer," *Proceedings of the Royal Society of London A: Mathematical, Physical and Engineering Sciences*, vol. 400, no. 1818, pp. 97–117, 1985.

[17] P. W. Shor, "Algorithms for quantum computation: discrete logarithms and factoring," in *Proceedings of the 35th IEEE Annual Symposium on Foundations of Computer Science*, Santa Fe, New Mexico, November 1994.

[18] L. K. Grover, "A fast quantum mechanical algorithm for database search," in *Proceedings of the 28th Annual ACM Symposium on the Theory of Computing*, ACM, May 1996.

[19] K.-H. Han and J.-H. Kim, "Quantum-inspired evolutionary algorithm for a class of combinatorial optimization," *IEEE Transactions on Evolutionary Computation*, vol. 6, no. 6, pp. 580–593, 2002.

[20] T. Gramß, S. Bornholdt, M. Groß, M. Mitchell, and T. Pellizzari, "The theory of quantum computation: an introduction," in *Non-Standard Computation: Molecular Computation—Cellular Automata—Evolutionary Algorithms—Quantum Computers*, chapter 5, pp. 141–178, Wiley-VCH, New York, NY, USA, 1998.

[21] P. Aliferis, "An introduction to reliable quantum computation," http://arxiv.org/abs/1107.2148.

[22] M. Şahin and M. Tomak, "The self-consistent calculation of a spherical quantum dot: a quantum genetic algorithm study," *Physica E: Low-Dimensional Systems and Nanostructures*, vol. 28, no. 3, pp. 247–256, 2005.

[23] M. Şahin, Ü. Atav, and M. Tomak, "Quantum genetic algorithm method in self-consistent electronic structure calculations of a quantum dot with many electrons," *International Journal of Modern Physics C*, vol. 16, no. 9, pp. 1379–1393, 2005.

[24] S. Dey, S. Bhattacharyya, and U. Maulik, "Quantum inspired genetic algorithm and particle swarm optimization using chaotic map model based interference for gray level image thresholding," *Swarm and Evolutionary Computation*, vol. 15, pp. 38–57, 2014.

[25] J.-C. Lee, W.-M. Lin, G.-C. Liao, and T.-P. Tsao, "Quantum genetic algorithm for dynamic economic dispatch with valve-point effects and including wind power system," *International Journal of Electrical Power & Energy Systems*, vol. 33, no. 2, pp. 189–197, 2011.

[26] J. G. Vlachogiannis and J. Østergaard, "Reactive power and voltage control based on general quantum genetic algorithms," *Expert Systems with Applications*, vol. 36, no. 3, pp. 6118–6126, 2009.